KSCE Journal of Civil Engineering (2016) 20(3):1099-1108

DOI 10.1007/s12205-016-0741-9

Sustainable Urban Transportation System

pISSN 1226-7988, eISSN 1976-3808
www.springer.com/12205

Modeling Lane Formation in Pedestrian Counter Flow and Its Effect on Capacity

Jooyong Lee*, Taewan Kim, Jin-Hyuk Chung***, and Jinho Kim******

Received September 13, 2015/Accepted January 25, 2016

Abstract

For the development of a sustainable transportation system, a modal shift from automobiles to walking or transit is encouraged. In order to design a more convenient and comfortable walking environment, a sound modeling of pedestrian flow is necessary. Most of the previously developed pedestrian flow models well described the macroscopic features of unidirectional pedestrian flow. However, in pedestrian counter-flow, interactions among conflicting pedestrians are so complicated and existing flow models fall short in explaining some features of pedestrian behaviors. A spontaneous lane formation, which helps to reduce conflicts and increase travel speeds, is a commonly observed feature of a crowded pedestrian flow. This paper develops a social-force based pedestrian model, which can explain the lane formation phenomenon. From the simulation results, it turns out that the 'following effect' and 'evasive effect' mainly contribute to the lane formation. Higher capacity and travel speed are obtained when pedestrians are more congregated.

Keywords: *sustainable transportation, social-force model, pedestrian flow, walking, cellular automata*

1. Introduction

For the development of a sustainable transportation system, a modal shift from automobiles to walking or transit is encouraged (Kim and Ulfarsson, 2008; Ha *et al.*, 2011; Kim *et al*., 2013; Lee and Park, 2014; Henao *et al.*, 2015; Piatkowski *et al*., 2015). One of the strategies to boost the modal shift is to provide a more convenient and comfortable walking environment, which requires sound understanding and modeling of pedestrian behaviors, especially for the design and operation of pedestrian facilities. Compared to the numerous vehicle motion models developed since 1930s, (Greenshields, 1934; Lighthill and Whitham, 1955; Gazis *et al*., 1959; Benekohal and Treiterer, 1988; Newell, 2002), pedestrian models are relatively recent and a few. Models of pedestrian flow have adopted two different approaches; one considers pedestrians as a fluid-like medium (Henderson, 1971) and the other considers pedestrians as a set of individual agents (Helbing and Molnár, 1995; Blue and Adler, 1998). Henderson (1971) has measured speed-density distribution functions for crowd fluids and a good agreement is obtained with Maxwell-Boltzmann theory. However, despite this analogy, the fluid dynamic approach falls short in describing microscopic characteristics of individual pedestrians such as frequent path change and conflict avoiding movements, so accordingly much attention has been paid to the agent-based approach.

The agent-based model consists of a social-force model and a cellular automata model. The earliest force model was proposed by Okazaki (1979), who has developed a magnetic force model to analyze pedestrian movements adopting a motion equation in magnetic fields. In 1995, Helbing and Molnár proposed a so-called social-force model which assumes that pedestrian movements are affected by external conditions, internal motivations, and random errors. The social-force model describes the movements of pedestrians with a force vector composed of a vector pointing towards the pedestrian's destination and repulsive force to avoid close contacts with other pedestrians. Because the social-force model can reproduce significant features of pedestrian flow and is flexible enough to incorporate many factors that affect pedestrian movements, many researchers developed their own social-force models (Hoogendoorn, 2003; Johansson and Helbing, 2008; Parisi *et al*., 2009; Chraibi *et al.*, 2010).

Cellular automata model divides pedestrian space into small fixed cells and a pedestrian who occupies one cell at a time can move to other cells by intuitively predetermined movement rules. In vehicular movement, the cellular automata model already has been applied and shown to be a good approximation of the macroscopic features of traffic flow, while maintaining its simplicity (Nagel and Schreckenberg, 1992; Krauss *et al*., 1997). Application of cellular automata models in pedestrian flows also began in the late 1990s. Blue and Adler (1998) have applied the

*Member, Researcher, Dept. of Urban Engineering, Chung-Ang University, Seoul 06974, Korea (E-mail: jylee3302@gmail.com)
**Member, Professor, Dept. of Urban Engineering, Chung-Ang University, Seoul 06974, Korea (Corresponding Author, E-mail: twkim@cau.ac.kr)
***Member, Professor, Dept. of Urban Planning and Engineering, Yonsei University, Seoul 03722, Korea (E-mail: jinchung@yonsei.ac.kr)
****Senior Researcher, Smart Station Research Team, Korea Railroad Research Institute, Uiwang 16105, Korea (E-mail: ziminpa@krri.re.kr)

cellular automata model onto unidirectional pedestrian flow and have shown that the fundamental diagram derived from pedestrian simulation is similar to the fundamental diagram of vehicular traffic. Extended analyses of cellular automata based pedestrian flow include Muramatsu *et al.* (1999), Blue and Adler (2001), Tajima *et al.* (2002), Isobe *et al.* (2004), Guo and Huang (2012).

Whether it is through the social-force model or the cellular automata model, the main concerns of the researchers are to simulate as closely as possible the real features of pedestrian movement. The features that characterize pedestrian movement which differ from vehicular movements are 1) pedestrians can move in a two-dimensional space (no exclusively designated lane for one direction movement) 2) counter-flows co-exist in the same space and collision avoidance is dependent upon individual's discernment. Recently, simulating pedestrian counter-flow has attracted considerable attention. Lam *et al.* (2002) have found that flow composition affects the capacity and speed of pedestrian flows in both direction. Takimoto *et al*. (2002) investigated the effects of a partition line in pedestrian counter-flow and have shown that the partition line enhances the critical density. These results suggests that pedestrian counter-flow is more inefficient than unidirectional flow because of the conflicts between opposing direction pedestrians. However, recent studies on counter-flow show contradicting results that counter-flow can be more efficient than unidirectional flow. Zhang *et al*. (2012) observed that the bidirectional fundamental diagram is insensitive to flow composition around high densities, which can be explained by the spontaneous formation of lanes that helps to reduce the conflicts. In fact, the effects of lane formation was already observed by Helbing *et al.* (2005), who have found through experiment that the bidirectional pedestrian flow rate can be higher than the unidirectional pedestrian flow rate for similar densities. Flötteröd and G., Lämmel (2015) have derived a bidirectional fundamental diagram through micro-simulation and argued that "bidirectional flows with lane formation being more efficient than unidirectional flows and bidirectional flows without lane formation being less effective than unidirectional flows".

Lane formation is an interesting phenomenon that characterizes pedestrian flow. It would be a natural and intuitive measure to avoid jamming transition and maintain free flow travel speed even in a dense counter-flow. The objective of this paper is to understand the effects of lane formation on the pedestrian flow characteristics. To this end, we first develop a modified social-force model with evasive effect and following effect which, we consider, are specific human behavioral elements that contribute to the lane formation. And then, through simulation of the modified social-force model, we analyze the effects of lane formation on the capacity and travel speed of pedestrian flow.

2. Model Development

The pedestrian model to be developed in this paper is based on the 'generalized-force model' by Helbing *et al*. (2000).

$$m_i \frac{dv_i}{dt} = \frac{v_i^0(t)e_i^0(t) - v_i(t)}{\tau_i} + \sum_{j(\neq i)} \boldsymbol{f}_{ij} + \sum_W \boldsymbol{f}_{iW} \tag{1}$$

This model assumes that a pedestrian's movement in a crowd, N, is determined by a mixture of socio-psychological and physical forces. The pedestrian i of mass m_i wants to move with a certain desired speed v_i^0 in a certain direction $\boldsymbol{e}_i^0$, generally which is the destination direction. Therefore the acceleration that the pedestrian would resume after a certain characteristic time τ would be $\frac{dv_i}{dt} = \frac{v_i^0(t)e_i^0(t) - v_i(t)}{\tau_i}$. However, at the same time, the pedestrian may tend to maintain a velocity-dependent distance from another pedestrian j and walls W. To include this tendency as the 'interaction forces', $\boldsymbol{f}_{ij}$ and $\boldsymbol{f}_{iW}$ are added at the second and third right-hand side terms of eq. (1). The interaction forces can be explained as follows. The tendency that two pedestrians (i and j) want to stay away from each other can be expressed as a repulsive force

$$A_i \exp[(r_{ij} - d_{ij})/B_i] n_{ij} \tag{2}$$

where A_i and B_i are coefficients, $r_{ij} = (r_i + r_j)$, r_i and r_j are the radius of pedestrian i and j, respectively, $d_{ij} = \|\boldsymbol{s}_i - \boldsymbol{s}_j\|$, $\boldsymbol{s}_i$ and $\boldsymbol{s}_j$ are the position of pedestrian i and j, respectively, and $\boldsymbol{n}_{ij} = (n_{ij}^1, n_{ij}^2) = (\boldsymbol{s}_i - \boldsymbol{s}_j)/d_{ij}$ is the normalized vector pointing from pedestrian j to i. When the pedestrians contact each other, in other words, $d_{ij} < r_{ij}$, the model assumes two additional forces, a 'body force' counteracting body compression and a 'sliding friction' impeding relative tangential force. These two forces are represented as $\varphi(r_{ij} - d_{ij})\boldsymbol{n}_{ij}$ and $\omega(r_{ij} - d_{ij})\Delta v_{ji}^t \boldsymbol{t}_{ij}$, respectively, where $\boldsymbol{t}_{ij} = (-n_{ij}^2, n_{ij}^1)$, $\Delta v_{ji}^t = (v_j - v_i) \cdot \boldsymbol{t}_{ij}$, φ and ω are constants. Finally, the interaction force can be represented as

$$\boldsymbol{f}_{ij} = \{A_i \exp[(r_{ij} - d_{ij})/B_i] + \varphi g(r_{ij} - d_{ij})\} \boldsymbol{n}_{ij} + \omega g(r_{ij} - d_{ij}) \Delta v_{ij}^t \boldsymbol{t}_{ij} \tag{3}$$

where the function $g(x)$ is zero when $x < 0$ and is x when $x > 0$.

Analogously, the interaction with the walls can also be represented as follows.

$$\boldsymbol{f}_{iW} = \{A_i \exp[(r_i - d_{iW})/B_i] + \varphi g(r_i - d_{iW})\} \boldsymbol{n}_{iW} - \omega g(r_i - d_{iW}) (v_i \cdot \boldsymbol{t}_{iW}) \boldsymbol{t}_{iW} \tag{4}$$

where $\boldsymbol{n}_{iW}$ denotes the direction perpendicular to the wall, $\boldsymbol{t}_{iW}$ the direction tangential to the wall and A_i, B_i are coefficients.

In the Helbing model, pedestrians basically tend to move towards their destination, where there are less conflicts with adjacent pedestrians. That is, only repulsive force is considered to account for the interaction between pedestrians. This assumption might be well fitted in the 'Escape panic' situation, which is originally intended for Helbing model. When panicking pedestrians rush over toward the exit, they would not fully consider the conflict of each other, indicating that their goal might be to leave the panic situation itself. Therefore, relying only on repulsive force was acceptable in the Helbing model to explicate its intended panic situations.

However, in a pedestrian counter-flow with normal situation, the same destination pedestrians intuitively tend to congregate,

which helps to avoid conflicts with opposite pedestrians and proceed without friction. We assume that this congregation effect is a direct cause of lane formation that makes the pedestrians flow more efficiently. To account for the congregation effect, we assume that pedestrians consider the position, movement direction, and the distance of adjacent pedestrians traveling to the same/opposite direction and then determine their paths ahead.

In this paper, we have added 'Following effect' and 'Evasive effect' to the original Helbing model to explain the pedestrian counter-flow. These two effects account for the behavior of pedestrians to follow others, while avoiding those who are opposing them. There are several researches, which have included these effects in order to depict the flow of moving objects like pedestrians, army ants, and so on (Burstedde *et al*., 2001; Couzin *et al*., 2003; Ko *et al*., 2013, Shuaib *et al*., 2013).

These effects are added in the present model by considering the 'moving direction' and 'relative displacement' of other pedestrians. The moving direction refers to the unit vector that is pointing towards the pedestrian's direction of movement. It is required to understand how a pedestrian would move in the near future. On the other hand, relative displacement means the difference of each pedestrian's current location. It is necessary for obtaining the present position of pedestrians in order to follow or evade. By considering both moving direction and relative displacement, the present model is able to depict the behavior of pedestrians more comprehensively.

2.1 Following Effect

When the pedestrian flow is crowded, the space that a pedestrian i can move would be limited and so he/she tends to follow the motions of the pedestrians ahead. In most cases, the pedestrians located behind the pedestrian i would rarely affect i's movement. We assume that the pedestrian is following the direction of other pedestrians located ahead, who have the same destination with him/her. We also suppose that the tendency to follow the direction of others would be higher if the pedestrian to follow is located closer to him/her. If we denote the unit velocity vector of the same destination pedestrian j as $\boldsymbol{v}_j$, the force that pedestrian i would like to follow the direction of pedestrian j is

$$C_i \exp[(r_{ij}-d_{ij})/D_i]v_j \tag{5}$$

C_i and D_i are coefficients which need to be calibrated. If we assume that pedestrian i's movement is not affected by the moving direction of pedestrian j (that is v_j) but by the relative displacement between pedestrian i and j, Eq. (5) can be transformed to

$$E_i \exp[(r_{ij}-d_{ij})/F_i]\,\boldsymbol{follow}_i^{l\text{ or }r} \tag{6}$$

where $\boldsymbol{follow}_i^{l\text{ or }r}$ is a unit vector perpendicular to pedestrian i's unit velocity vector, v_i. According to the relative displacement, whether pedestrian j is located on the left-side or right-side of pedestrian i's direction, this force leads pedestrian i to steer his/her direction to follow the leader, pedestrian j. E_i and F_i are coefficients which need to be calibrated.

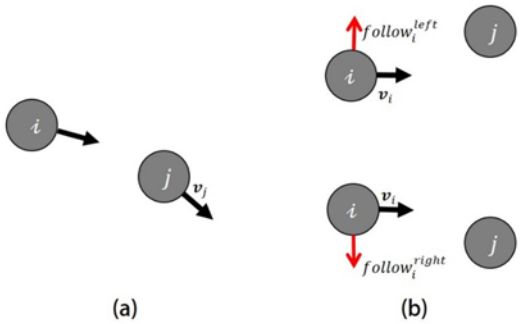

Fig. 1. Follow Effect to the Pedestrians in Same Direction: (a) Follow the Vector, (b) Follow the Location

The two following-effect forces are modeled to have a linear relationship, therefore the total following-effect force is

$$Follow\ effect_{ij} = \{C_i \exp[(r_{ij}-d_{ij})/D_i]v_j + E_i \exp[(r_{ij}-d_{ij})/F_i]\,\boldsymbol{follow}_i^{l\text{ or }r}\} \times d_j \tag{7}$$

where, $d_j = 1$ if pedestrian j has same destination with pedestrian i, and $d_j = 0$, otherwise.

2.2 Evasive Effect

In crowded conditions, a pedestrian not only follows the same direction pedestrian but also tends to evade the opposite direction pedestrian located in front of him. This evasive movement is often considered as an essential factor for determining the Level of Service (LOS) for a certain pedestrian flow. Kim *et al.* (2014) have defined five different evasive movements in pedestrian flow, and established criteria of determining the LOS regarding the number of evasive movements occurred. To model the evasive movement, we employ $\boldsymbol{ref}_j$ and $\boldsymbol{evade}_i^{l\text{ or }r}$.

The former, $\boldsymbol{ref}_j$, represents that pedestrian i would evade opposite pedestrian j according to the moving direction. That is, if the opposite pedestrian j's unit velocity vector is v_j, $\boldsymbol{ref}_j$ is the reflective vector of v_j where the normal-line is the direction of pedestrian i, v_i. This effect can be modeled as Eq. (8). C_i and D_i are coefficients which need to be calibrated.

$$C_i \exp[(r_{ij}-d_{ij})/D_i]\boldsymbol{ref}_j \tag{8}$$

The latter, $\boldsymbol{evade}_i^{l\text{ or }r}$, represents that pedestrian i's evasive movement is affected by the relative displacement between pedestrian i and j. The vector $\boldsymbol{evade}_i^{l\text{ or }r}$ is a unit vector perpendicular to pedestrian i's unit velocity vector, $\boldsymbol{v}_i$. It points to the right-side or left-side of pedestrian j's movement, according to the pedestrian i's location.

$$E_i \exp[(r_{ij}-d_{ij})/F_i]\boldsymbol{evade}_i^{l\text{ or }r} \tag{9}$$

$\boldsymbol{evade}_i^{l\text{ or }r}$ represents that pedestrian i is heading to the direction which would lead him/her to evade pedestrian j. E_i and F_i are coefficients which need to be calibrated.

An interesting situation is when the pedestrians i and j are located in direct opposite of each other. Since there is no angle of

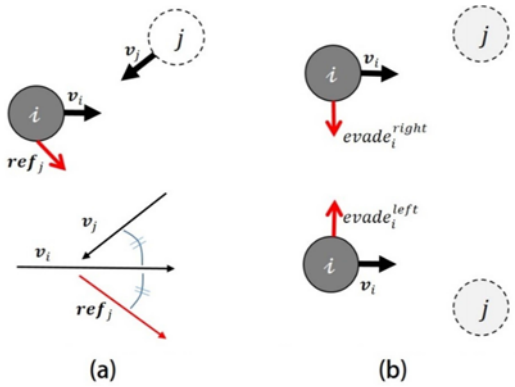

Fig. 2. Evasive Effect to the Pedestrians in Opposite Direction: (a) Evade by Vector, (b) Evade by Location

incidence, $\boldsymbol{ref}_j$ would be impractical to simulate evasive movements. In this case, we have modeled $\boldsymbol{evade}_i^{l\text{ or }r}$ to direct to the right-side or left-side randomly. This assumption is acceptable because, when there is no information for one to decide on which side to evade, it would be practical for one to evade by chance.

Therefore the total evasive-effect force is

$$Evasive\ \ effect_{ij} = \{C_i \exp[(r_{ij}-d_{ij})/D_i]\boldsymbol{ref}_j + E_i \exp[(r_{ij}-d_{ij})/F_i]\boldsymbol{evade}_i^{l\text{ or }r}\} \times d_j' \tag{10}$$

where, $d_j' = 1$ if pedestrian j has different destination with pedestrian i, and $d_j' = 0$, otherwise.

2.3 Overall Model

In the original Helbing model, the interaction force has been limited to only repulsive force, regardless of direction. However, the pedestrian in present model has additional terms, following effect and evasive effect. The following effect is adjusted to those who have the same destination, while the evasive effect is adjusted to the pedestrians who have opposite destination. Finally, the modified social-force model is represented as

$$m_i\frac{dv_i}{dt} = m_i\frac{v_i^0(t)e_i^0(t)-v_i(t)}{\tau_i} + \sum_{j(\neq i)}\{\boldsymbol{f}_{ij} + Follow\ \ effect_{ij} + Evasive\ \ effect_{ij}\} + \sum_W \boldsymbol{f}_{iW} \tag{11}$$

Where,

$$\boldsymbol{f}_{ij} = \{A_i' \exp[(r_{ij}-d_{ij})/B_i] + \varphi g(r_{ij}-d_{ij})\}\boldsymbol{n}_{ij} + \omega g(r_{ij}-d_{ij})\Delta v_{ji}^t \boldsymbol{t}_{ij}$$

$$Follow\ \ effect_{ij} = \{C_i \exp[(r_{ij}-d_{ij})/D_i]v_j + E_i \exp[(r_{ij}-d_{ij})/F_i]\boldsymbol{follow}_i^{l\text{ or }r}\} \times d_j$$

$$Evasive\ effect_{ij} = \{C_i \exp[(r_{ij}-d_{ij})/D_i]\boldsymbol{ref}_j + E_i[(r_{ij}-d_{ij})/F_i]\boldsymbol{evade}_i^{l\text{ or }r}\} \times d_j'$$

The coefficient A_i in the original interaction force ($\boldsymbol{f}_{ij}$) has been replaced by A_i', which needs to be calibrated also. This change of coefficient is to balance the additional two effects developed in this paper.

3. Calibration of the Coefficients

The coefficients of the model are calibrated by Genetic Algorithm to emulate the real-world pedestrian flow. We have used the data acquired by Zhang *et al.* (2012) (The authors gratefully acknowledge for sharing the data, and it is publicly shared at http://www.asim.uni-wuppertal.de/datenbank/own-experiments/corridor/2d-bidirectional.html), which has been experimented in Germany, 2009. Zhang *et al.* (2012) have observed pedestrians walking in an 8 m length, 3.6 m width walkway, and have collected the data of pedestrian ID, unit time (0.0625s), and each pedestrian's x, y, z coordinates. The data set used in calibration was named as 'BFR-DML-360-075-075' by

Table 1. Traffic Situation and Geometric Condition

Pedestrians heading Left	Pedestrians heading Right	Geometry
Number: 62 pedestrians Flow rate: 32 ped/min/m	Number: 65 pedestrians Flow rate: 34 ped/min/m	Flat walkway (Length 8 m, Width 3.6 m)

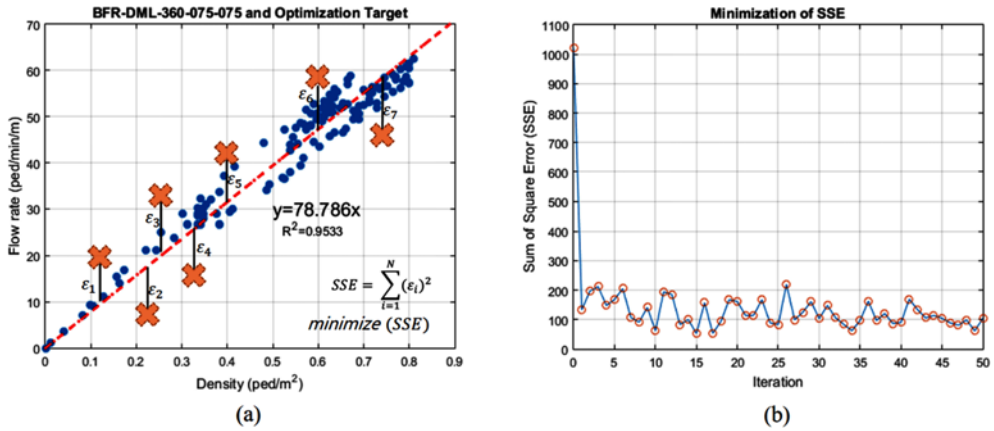

Fig. 3. Data Used for Calibration (a) and Minimization of SSE (b)

Table 2. Calibration Result of Each Coefficient

	A_i'	C_i	D_i	E_i	F_i
Calibration Result	1,632	12	0.35	500	0.82

Zhang *et al.* (2012).

With this data, we have obtained the density-flow rate relationship (fundamental diagram) of the experiment. Since the fundamental diagram shows the basic characteristics of the traffic flow, it would be suitable if the present model produces the fundamental diagram analogous to that of experimental data. In this sense, the present model has been set to the same traffic situation and geometric condition as the experimental data, listed in Table 1. The resemblance between simulation results and experimental data would support that the present model emulates the traffic flow in real-world. The entrance of pedestrians for both directions are assumed to follow Poisson distribution.

The calibration has been conducted to obtain optimal coefficients such that the model's fundamental diagram best fits to the experimental data. This could be achieved by minimizing the Sum of Square Errors (SSE) of a linear regression with the present model and experimental data, as shown in Fig. 3(a). The range of each coefficient for calibration varied by A_i' being 1,500~2,000, C_i and E_i being 0~500, D_i and F_i being 0~1. Moreover, A_i', C_i and E_i have been rounded to the nearest integer, while D_i and F_i were rounded to the nearest second decimal. The condition of genetic algorithm has been set for 30 population size, ranking selection with 60% survival rate, 10% mutation rate and 50 iterations. In Fig. 3(b), the SSE has been stabilized between iteration 43~50, so we have chosen the coefficients of iteration 50, as in Table 2.

4. Validation and Simulation Analysis

4.1 Validation

The fundamental diagrams of the Helbing model, experimental data, and present model are depicted in Fig. 4. The fundamental diagram of the present model turned out to be analogous to that of the experimental data. The density and flow rate of two data are distributed analogously, and the speed, which is the gradient of the fundamental diagram, were both calculated as about 1.3 m/s. This result implies that the present model has realistically emulated the pedestrian flow in the real-world.

However, the result of the Helbing model indicates that there existed more traffic jam compared to the real-world data and present model. The maximum density reached up to 2 ped/m^2,

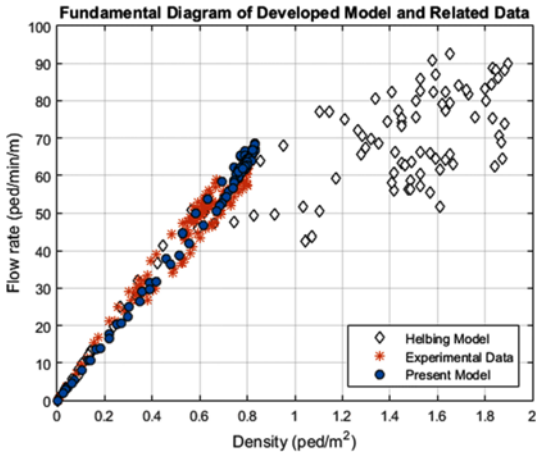

Fig. 4 Fundamental Diagram of Present Model and Related Data

while the flow rate appeared to be 90 ped/min/m in maximum. The speed of the Helbing model has been calculated lower than the present model's one. This implies that the Helbing model has experienced more traffic congestion than the other two results. These differences were thought to be affected by additional effects included in the present model. We have determined that the following and evasive movements helped pedestrians avoid conflict between each other, which had improved the overall traffic condition of the walkway. Moreover, since the model has been calibrated with real-world data, the present model seems to have emulated the real-world pedestrians more effectively.

Another validation process has been conducted by comparing the statistical estimates of the present model and experimental data. In this process, the performance of the present model could be statistically analyzed by repeating each simulation for 200 times. We have obtained the mean and variance of flow rate, speed and density as listed in Table 3. Then, the estimates of the present model and the Helbing model are compared with the values obtained by real-word experiment.

The mean values of the present model were calculated to be more similar to the result of real-world data than the mean values of the Helbing model. Also, the variances of the present model were smaller than that of the Helbing model. Meanwhile, the Helbing model had higher flow rates and lower speed and density compared to the present model, which also implies that the Helbing model has experienced statistically significant traffic jam compared to the present model.

4.2 Model Performance

In the validation process, both the following effect and evasive

Table 3. Statistical validation of Present Model

	Real-world	Present Model		Helbing Model	
		Mean	Variance	Mean	Variance
Flow rate (ped/min/m)	42.76	40.89	3.33	46.55	16.31
Speed (m/s)	1.3	1.10	0.0038	0.93	0.0111
Density (ped/m^2)	0.53	0.53	0.0026	0.9	0.032

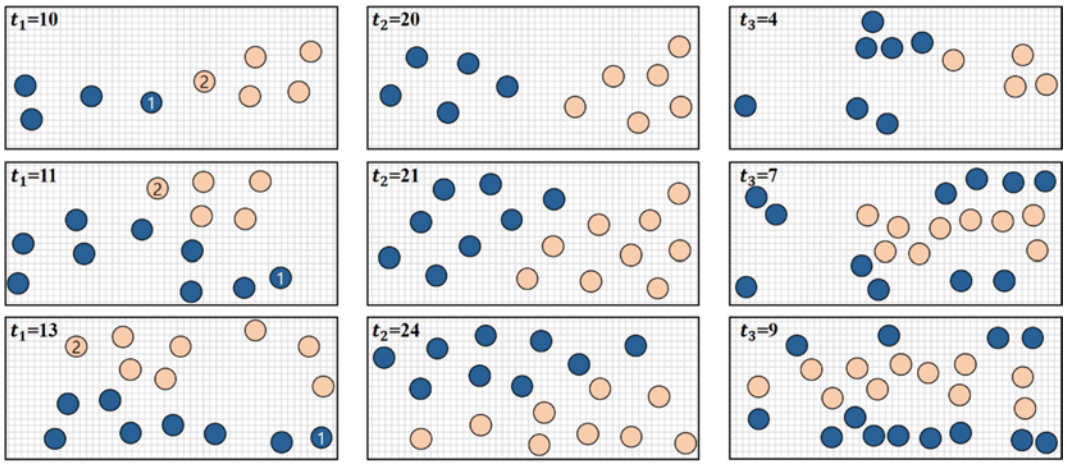

Fig. 5. Evasive Movement and Following Pedestrians in Various Situations

effect were thought to be responsible for the improvement. These effects were influencing the pedestrians to avoid the conflict of each other and advance toward the destination more easily as seen through the snapshots of our simulation in Fig. 5.

In Fig. 5(a), pedestrian counter-flow of each heading to the right and left are imminent to collision when the unit time (t_1) is 10. However, the pedestrian labeled as '1' reacts mainly to the nearest opposite pedestrian '2', while the pedestrian '2' also takes account of the opposite pedestrian '1', respectively. The evasive effect leads to both pedestrians changing their route to avoid collision. Moreover, other pedestrians that were following pedestrian '1' and '2' also avoid the collision as well. This has been achieved by the following effect. When unit time (t_1) is 11, pedestrians who were heading to the same destination with pedestrian '1' follow the leader by moving to the right-side of the walkway. Similarly, opposite pedestrians including '2' also move to the right-side. This results in the formulation of a spontaneous lane of pedestrian flow in unit time (t_1) 13.

Of course, the 'Keep Right' rule was not included in the present model, so such right-sided lane was just a coincidence. Nonetheless, the formation of lanes has been generally emulated, whether people were located on the right-side or left-side of the walkway. Fig. 5(b) and Fig 5(c) show these cases where left-sided lane or formation of three lanes occurred. In this context, lane formation is expected to increase the overall capacity.

To investigate the effect of lane formation for different directional flow rate, we have tested five different flowrate ratios, 1:9, 2:8, 3:7, 4:6, and 5:5. Regarding four traffic characteristics, the results are presented in Table 4. While the three characteristics (flow rate, speed and density) are well established indicators for determining the traffic, a newly suggested value, 'Collision', has been adopted in this paper. We have defined the pedestrians to have experienced a collision when the distance with any other pedestrian is under 0.1 m. Then, the number of collisions per pedestrian during the simulation has been regarded as the traffic characteristic 'Collision'.

Kim *et al.* (2014) have found that the lateral distance of personal space is 0.49 m, while the longitudinal distance is 0.65 m in Korea. The Korean Highway Capacity Manual (2013) also defines the personal space of pedestrian to be 0.2 m^2. In this sense, it is acceptable to assume that a pedestrian has experienced collision by being closer than 0.1m with any other pedestrian. The mean and variance of each characteristic have been obtained by repeating each simulation 10 times.

According to Table 4, when the flow rate ratio is heavily imbalanced (like the 1:9 scenario), there are little differences in the mean of flow rate, speed and density between the present model and the Helbing model. However, when the flow rate ratio is more equivalent (as the 5:5 scenario), the speed of the Helbing model is lower than the speed of the present model, while the density of the Helbing model is higher than the density of the present model. This implies that the Helbing model experienced more traffic congestion than the present model

By altering the flow rate ratio from the imbalanced to the equivalent scenario, the mean collision of the present model has remained stable around 10, which indicates that the pedestrians in the present model have experienced a stabilized travel regardless of flow rate ratio. Moreover, the variance of collision in the present model has generally decreased. To sum up, the pedestrians in the present model had uniform collision while its variance became smaller when the flow rate ratio became equivalent.

Overall results in Table 4 imply that in unidirectional pedestrian flow, lane formation occurs rarely in both models, indicating little difference between the two models. However, in a bidirectional counter-flow, the present model can well replicate the phenomenon of lane formation.

Meanwhile, lane formation could be quantitatively analyzed by the 'Order Parameter'. Here, we have adopted the order parameter used by Delhommelle (2005) to detect the formation of lanes in driven liquids and colloids. The value of ϕ_i is equal to 1 for a given pedestrian i, if the distance between i and opposite pedestrian j is larger than the distance between two nearest

Table 4. Traffic Characteristics According to the Flow Rate Ratio

Traffic characteristics		Flow rate ratio	1:9	2:8	3:7	4:6	5:5
Flow rate (ped/min/m)	Mean	Present	13.29	22.82	32.73	37.47	41.34
		Helbing	13.02	25.28	35.89	39.89	42.00
	Variance	Present	188.59	317.59	459.85	515.63	637.87
		Helbing	265.31	384.40	465.51	591.50	665.61
Speed (m/s)	Mean	Present	1.18	1.22	1.17	1.16	1.09
		Helbing	1.10	1.01	0.86	0.76	0.71
	Variance	Present	0.11	0.09	0.16	0.18	0.22
		Helbing	0.11	0.13	0.12	0.12	0.12
Density (ped/m^2)	Mean	Present	0.17	0.29	0.42	0.47	0.53
		Helbing	0.20	0.44	0.80	1.01	1.08
	Variance	Present	0.03	0.05	0.07	0.08	0.10
		Helbing	0.08	0.18	0.37	0.55	0.60
Collision (#)	Mean	Present	11.49	10.71	10.78	8.92	10.15
		Helbing	2.69	7.60	25.83	51.65	51.55
	Variance	Present	201.40	185.01	165.04	71.66	86.86
		Helbing	33.35	180.73	759.12	2251.22	2041.75

neighbors of i heading to the same destination. Otherwise, ϕ_i is equal to 0. The order parameter in any unit time t is defined to be $\phi^t = \sum_{i=1}^{N} \phi_i / N$, with N being the number of total pedestrians present. Then, the global order parameter (ϕ) in a single run of simulation has been obtained by the weighted mean of each ϕ^t with the existing pedestrian amount (N) in each unit time. The order parameter is close to 1 when the formation of lane had occurred strongly.

However, Nowak and Schadschneider (2012) have pointed out that this value is generally larger than 0, even though when every pedestrian is distributed randomly. To overcome this shortcoming, they have revised the order parameter with Eq. (12), which uses the mean order parameter (ϕ_0) when every pedestrian is randomly distributed. In this paper, randomly distributed pedestrians were simulated for 10,000 times and the mean order parameter of these simulations were defined to be ϕ_0 ($\phi_0 = 0.1883$). In this context, order parameters are scaled to revise randomly distributed pedestrians and lane formation could be quantitatively analyzed.

$$\phi := \frac{\phi - \phi_0}{1 - \phi_0} \tag{12}$$

In Fig. 6(a), the order parameters according to each flow rate ratio are depicted for both models. These values were obtained by the mean of order parameters in the equal simulations, which were used in Table 4. The order parameter of the present model has been analyzed to be large enough, and it has increased steadily by altering the flow rate ratio. This result supports the formerly mentioned inference that the present model's improvement in Table 4 has been caused by a strong lane formation. Under an imbalanced flow rate ratio, the present model had a relatively small order parameter. However, the order parameter increased when flow rate ratio became equivalent, which helped the present

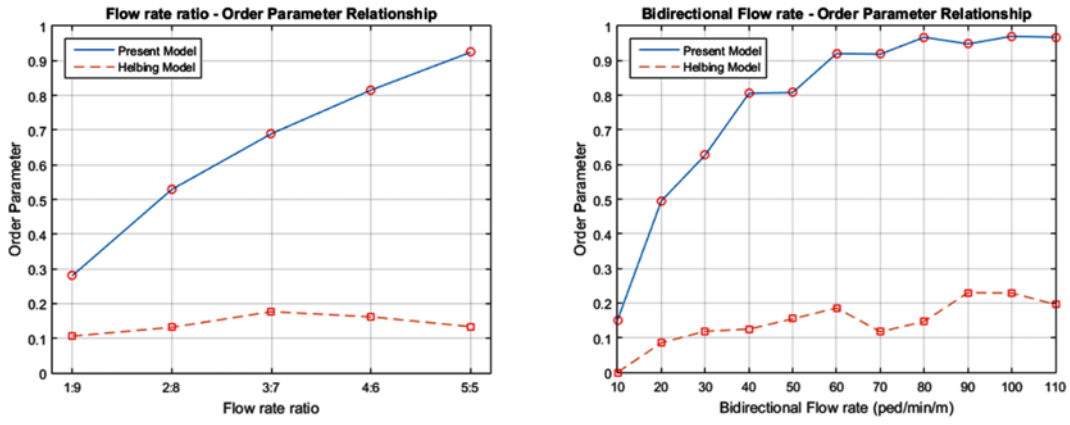

(a) (b)

Fig. 6. Order Parameter for Different Flow Rate Ratio (a) and Bidirectional Flow Rate (b)

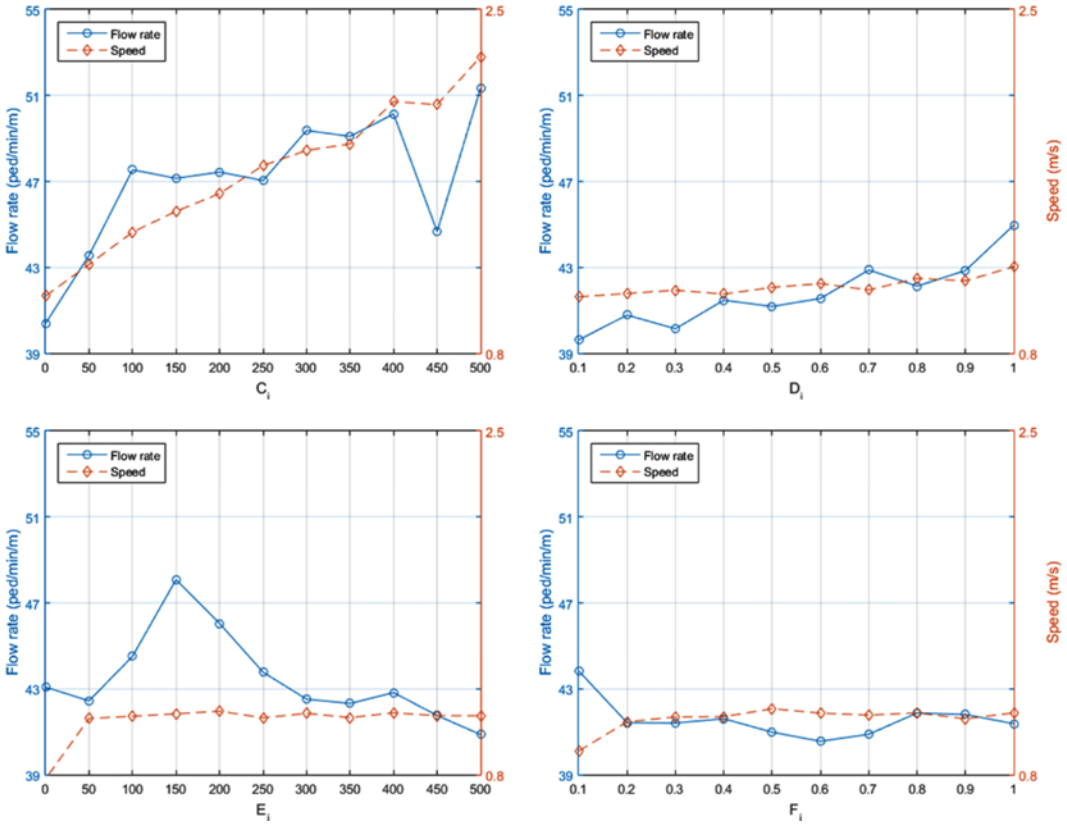

Fig. 7. Sensitivity Analysis in Regard with Flow Rate and Speed

model to reproduce good results. Therefore, strong formation of lane in the present model is thought to be responsible for the improvement mentioned earlier in Table 4.

In a further analysis, the formation of lane had strongly occurred in the present model by not only altering the flow rate ratio, but also by increasing the bidirectional flow rate itself with the flow rate ratio fixed to 5:5. In Fig. 6(b), the increase of bidirectional flow rate had generally led the order parameter to increase. Below 40 ped/min/m bidirectional flow rate, the order parameter of the present model has increased sharply. However, when the bidirectional flow rate was larger than 40 ped/min/m, it increases gradually and finally becomes steady around 0.95 over 80 ped/min/m. This is reasonable since the increase of bidirectional flow rate would lower the amount of spare-spaces that would be necessary to form lanes.

4.3 Sensitivity Analysis

In order to determine the impact of each coefficient, sensitivity analysis has been conducted. Since the characteristic of coefficient A_i' is well known for originally being adopted in the Helbing model, the other four coefficients (C_i, D_i, E_i and F_i) were considered in this analysis. Sensitivity analysis has been conducted by changing the target coefficient, while the other coefficients were fixed as the default value obtained by calibration. The range of coefficients were the same used in the calibration process, and the results were obtained by running the simulation 10 times and taking the mean value.

According to Fig. 7, flow rate was most sensitive to C_i, followed by D_i. Since those coefficients were used with 'moving direction', it seems that the flow rate is more sensitive to the moving direction than the relative displacement of other pedestrians. However, speed was only sensitive to C_i, compared to the other three coefficients. In conclusion, we have determined that pedestrian flow is more sensitive to the differences in moving direction, rather than the relative displacements of pedestrians.

5. Conclusions

A newly developed social force model is proposed to investigate the effects of lane formation in a pedestrian counter-flow. The calibration was conducted by utilizing the genetic algorithm, and it has been validated that the present model emulates the real-world pedestrian flow well. The present model shows that the following effect and evasive effect contribute to lane formation. From the simulation, we have found that lane formation reduced the density and collision, while increasing the speed.

Lane formation had little impact when the flow rate ratio was imbalanced. On the other hand, it had a stronger impact when the directional flow rate ratio was equivalent, and traffic flow was heavier. By the sensitivity analysis, pedestrian flow was more sensitive to the differences in moving direction than the relative displacements of pedestrians.

Acknowledgements

This research was supported by the Chung-Ang University *Excellent Student Scholarship* and the grant from "Development of convenience improvement technology for passengers in the metro station (15RTRP-B067918-03)" funded by Ministry of Land, Infrastructure and Transport of Korean government.

References

Benekohal, R. F. and Treiterer, J. (1988). "CARSIM: Car-following model for simulation of traffic in normal stop-and-go conditions." *Transportation Research Record*, Issue 1194, pp. 99-111, (http://onlinepubs.trb.org/Onlinepubs/trr/1988/1194/1194-011.pdf)

Blue, V. J. and Adler, J. L. (1998). "Emergent fundamental pedestrian flows from cellular automata microsimulation." *Transportation Research Record*, Issue 1644, pp. 29-36, DOI: 10.3141/1644-04.

Blue, V. J. and Adler, J. L. (2001). "Cellular automata microsimulation for modeling bi-directional pedestrian walkways." *Transportation Research B*, Vol. 35, No. 3, pp. 293-312, DOI: 10.1016/s0191-2615(99)00052-1.

Burstedde, C., Klauck, K., Schadschneider, A., and Zittarz, J., (2001). "Simulation of pedestrian dynamics using a two-dimensional cellular automaton." *Physica A*, Vol. 295, Nos. 3-4 pp. 507-525, DOI: 10.1016/s0378-4371(01)00141-8.

Chraibi, M., Seyfreid, A., and Schadschneider, A. (2010). "Generalized centrifugal-force model for pedestrian dynamics." *Physical Review E,* Vol. 82, No. 4, 046111, DOI: 10.1103/physreve.82.046111.

Couzin, I. D. and Franks, N. R., (2003). "Self-organized lane formation and optimized traffic flow in army ants." *Proceedings of the Royal Society B: Biological Science*s, Vol. 270, No. 1511, pp. 139-146, DOI: 10.1098/rspb.2002.2210.

Delhommelle, J. (2005). "Should "lane formation" occur systematically in driven liquids and colloids?." *Physical Review E*, Vol. 71, No. 1, pp. 16705, DOI: 10.1103/physreve.71.016705.

Flötteröd, G. and Lämmel, G. (2015). "Bidirectional pedestrian fundamental diagram." *Transportation Research Part B*, Vol. 71, pp. 194-212, DOI: 10.1016/j.trb.2014.11.001.

Gazis, D. C., Herman, R., and Potts, R. B. (1959). "Car-following theory of steady-state traffic flow." *Operations Research*, Vol. 7, No. 4, pp. 499-505, DOI: 10.1287/opre.7.4.499.

Greenshields, B. D. (1934). "A study on traffic capacity." *Highway Research Board, Proc.,* Vol. 1935.

Guo, R. and Huang, H. (2012). "Formulation of pedestrian movement in microscopic models with continuous space representation." *Transportation Research C*, Vol. 24, pp. 50-61, DOI: 10.1016/j.trc.2012.02.004.

Ha, E., Joo, Y., and Jun, C. (2011). "An empirical study on sustainable walkability indices for transit-oriented development by using the analytic network process approach." *International Journal of Urban Sciences,* Vol. 15, No. 2, pp. 137-146, DOI: 10.1080/12265934.2011.615977.

Helbing, D. and Molnár, P. (1995). "Social force model for pedestrian dynamics." *Physical Review E*, Vol. 51, No. 5, pp. 4282-4286, DOI: 10.1103/physreve.51.4282.

Helbing, D., Buzna, L., Johansson, A., and Werner, T. (2005). "Self-organized pedestrian crowd dynamics: Experiments, simulations, and design solutions." *Transportation Science*, Vol. 39, No. 1, pp. 1-24, DOI: 10.1287/trsc.1040.0108.

Helbing, D., Farkas, I., and Vicsek, T. (2000). "Simulating dynamical features of escape panic." *Nature*, Vol. 407, No. 6803, pp. 487-490, DOI: 10.1038/35035023.

Henao, A., Piatkowski, D., Luckey, K., Nordback, K., Marshall, W., and Krizek, K. (2015). "Sustainable transportation infrastructure investment and mode share changes: A 20-year background of Boulder, Colorado." *Transport Policy*, Vol. 37, pp. 64-71, DOI: 10.1016/j.tranpol.2014.09.012.

Henderson, L. F. (1971). "The statistics of crowd fluids." *Nature,* Vol. 229, No. 5284, pp. 381-383, DOI: 10.1038/229381a0.

Hoogendoorn, S. P. (2003). "Walker behaviour modelling by differential games." *In Interface and Transport Dynamics. Springer Berlin Heidelberg*. pp. 275-294, DOI: 10.1007/978-3-662-07969-0_27.

Isobe, M., Adachi, T., and Nagatani, T. (2004). "Experiment and simulation of pedestrian counter flow." *Physics A*, Vol. 336, No. 3, pp. 638-650, DOI: 10.1016/j.physa.2004.01.043.

Johansson, A. and Helbing, D. (2008). "Analysis of empirical trajectory data of pedestrians." *Handbook of Pedestrian and Evacuation Dynamics, Part I*, pp. 203-214, DOI: 10.1007/978-3-642-04504-2_15.

Kim, S. and Ulfarsson, G. F. (2008). "Curbing automobile use for sustainable transportation: analysis of mode choice on short home-based trips." *Transportation*, Vol. 35, No. 6, pp. 723-737, DOI: 10.1007/s11116-008-9177-5.

Kim, S., Choi, J., and Kim, S. (2013). "Roadside walking environments and major factors affecting pedestrian level of service." *International Journal of Urban Sciences*, Vol. 17, No. 3, pp. 304-315, DOI: 10.1080/12265934.2013.825422.

Kim, S., Choi, J., Kim, S., and Tay, R. (2014). "Personal space, evasive movement and pedestrian level of service." *Journal of Advanced Transportation*, Vol. 48, No. 6, pp. 673-684, DOI: 10.1002/atr.1223.

Ko, M. S., Kim, T. W., and Sohn, K. M. (2013). "Calibrating a social-force-based pedestrian walking model based on maximum likelihood estimation." *Transportation*, Vol. 40, No. 1, pp. 91-107, DOI: 10.1007/s11116-012-9411-z.

Krauss, S., Wagner, P., and Gawron, C. (1997). "Metastable states in a microscopic model of traffic flow." *Physical Review E*, Vol. 55, No. 5, pp. 5597-5602, DOI: 10.1103/physreve.55.5597.

Lam, W., Lee, J., and Cheung, C. (2002). "A study of the bi-directional pedestrian flow characteristics at Hong-Kong signalized crosswalk facilities." *Transportation*, Vol. 29, No. 2, pp. 169-192,DOI: 10.1023/a:1014226416702.

Lee, H. S. and Park, E. Y. (2014). "Comparing the environment for elderly pedestrians among different-sized cities of Gyeonggi province in Korea." *International Journal of Urban Sciences*, Vol. 18, No. 1, pp. 76-89, DOI: 10.1080/12265934.2013.863449.

Lighthill, M. J. and Whitham, J. B. (1955). "On kinematic waves II; A theory of traffic flow on long crowd roads." *Proceedings of the Royal Society A*, Vol. 229, No. 1178, pp. 317-345, DOI: 10.1098/rspa.1955.0089.

Ministry of Land, Transport and Maritime Affairs, Korea (2013). "Korean highway capacity manual." pp. 618 (in Korean).

Muramatsu, M., Irie, T., and Nagatani, T. (1999). "Jamming transition in pedestrian counter flow." *Physica A,* Vol. 267, No. 3, pp. 487-498, DOI: 10.1016/s0378-4371(99)00018-7.

Nagel, K. and Schreckenberg, M. (1992). "A cellular automaton model for freeway traffic." *Journal of Physics I France*, Vol. 2, No. 12, pp. 2221-2229, DOI: 10.1051/jp1:1992277.

Newell, G. F. (2002). "A simplified car-following theory: A lower order model." *Transportation Research B*, Vol. 36, No. 3, pp. 195-205,

DOI: 10.1016/s0191-2615(00)00044-8.

Nowak, S. and Schadschneider, A. (2012). "Quantitative analysis of pedestrian counterflow in a cellular automaton model." *Physical Review E,* Vol. 85, No. 6, pp. 066128, DOI: 10.1103/physreve.85.066128.

Okazaki, S. (1979). "A study of pedestrian movement in architectural spaces, Part I: pedestrian movement by the application of magnetic models." *Trans. A. I. J.*, Vol. 283, pp. 111-119.

Parisi, D. R., Gilman, M., and Moldovan, H. (2009). "A modification of the social force model can reproduce experimental data of pedestrian flows in normal conditions." *Physics A*, Vol. 388, No. 17, pp. 3600-3608, DOI: 10.1016/j.physa.2009.05.027.

Piatkowski, D., Krizek, K., and Handy, S. (2015). "Accounting for the short term substitution effects of walking and cycling in sustainable transportation" *Travel Behaviour and Society,* Vol. 2, No. 1, pp. 32-41, DOI: 10.1016/j.tbs.2014.07.004.

Shuaib, M., Alia, O., and Zainuddin, Z. (2013). "Incorporating prediction factor into the investigation capability in the social force model: application on avoiding grouped pedestrians." *Applied Mathematics & Information Sciences*, Vol. 7, No. 1, pp. 323-331, DOI: 10.12785/amis/070141.

Tajima, Y., Takimoto, K., and Nagatani. T. (2002). "Pattern formation and jamming transition in pedestrian counter flow." *Physica A*, Vol. 313, No. 3, pp. 709-723, DOI: 10.1016/s0378-4371(02)00965-2.

Takimoto, K., Tajima, Y., and Nagatani, T. (2002). "Effect of partition line on jamming transition in pedestrian counter flow." *Physica A*, Vol. 308, No. 1, pp. 460-470, DOI: 10.1016/s0378-4371(02)00550-2.

Zhang, J., Klingsch, W., Schadschneider, A., and Seyfried, A. (2012). "Ordering in bidirectional pedestrian flows and its influence on the fundamental diagram." *Journal of Statistical Mechanics*, Vol. 2012, No. 2, pp. 02002, DOI: 10.1088/1742-5468/2012/02/p02002.